

**Computation of All Optimum Dyads in the
Approximate Synthesis of Planar Linkages for
Rigid-Body Guidance**

Jin Yao

Department of Mechanical Engineering

Sichuan Union University

Chengdu, P. R. China

Jorge Angeles (the corresponding author)

Department of Mechanical Engineering and Centre for Intelligent Machines

McGill University

817 Sherbrooke Street, Montreal, Canada H3A 2K6

Fax: (514) 398-7348

Abstract

The approximate synthesis of a planar four-bar linkage for rigid-body guidance consists in finding all the relevant parameters of the linkage that produces a set of the poses of its coupler link that best approximate a large number of the prescribed poses. By “large” we mean here a number larger than that allowing for an exact matching of poses. Moreover, the approximation error in the synthesis equations is measured in the least-square sense, the problem thus giving rise to an optimization problem. Each solution of this problem, producing a local minimum of the approximation error yields one dyad, the combination of any pair of these then yielding one linkage. While purely numerical methods yield only isolated local minima, we apply here the contour method in an attempt to finding all the real stationary points of the problem at hand. First, symbolic computations are used to derive the underlying *normal equations* of the optimization problem. The normal equations are then reduced to a set of two bivariate polynomial equations. These two equations are plotted in the plane of the two unknown variables, the two contours that they define in this plane being then overlapped. In principle, their intersections provide, visually, all the real solutions of the problem under study as well as the numerical conditioning of these solutions. Finally, numerical techniques are used to refine a solution to the desired accuracy. An example is included to illustrate the method.

1 Introduction

In most cases, both kinematic analysis and kinematic synthesis lead to a system of polynomial equations. There are in general two common tools for solving the kinematics equations, i.e., numerical methods and elimination methods. Numerically, a polynomial system is solved by providing an initial guess to an iterative method, usually of the Newton type. However, Newton methods entail diffi-

culties in that they depend on suitable initial guesses and provide one solution at a time. Recently, a technique known as polynomial continuation was developed [1], which can reliably compute all solutions to polynomial systems of moderate size. As to elimination methods, the multivariate polynomial system is reduced to one single univariate polynomial equation whose roots, real and complex, can be found with commercial software. These two methods have been applied to finding the roots of polynomial systems, in both kinematic analysis and kinematic synthesis [2–9]. Additional related references are listed in [10]. Elimination methods have become pervasive in kinematic analysis and synthesis by virtue of the commercial availability of highly reliable software for computer algebra. However, polynomial-continuation and elimination methods have been mostly confined to applications of exact synthesis, besides extensive applications in kinematic analysis. Approximate synthesis problems have been solved almost exclusively with purely numerical methods. The problem with these methods, nevertheless, is that their convergence is highly dependent on the choice of the initial guess, and can seldom be guaranteed; besides, when these methods do converge, they do so to a local optimum, the uncertainty of whether this optimum is global still remaining. To be sure, we can cite one case [11] in which a polynomial-continuation method was applied to the approximate synthesis of a planar four-bar linkage for path generation, with a prescribed timing of the points visited. The authors of the above reference derived a system of polynomial equations with a total degree of 343, which means that up to as many solutions of the polynomial system are to be expected.

On the other hand, recent advances in numerical, symbolic, and graphics software provide us with new powerful tools to solve the problem at hand by alternative means. One method, named the contour or semigraphical method, using a combination of symbolic and numerical computations as well as computer graphics tools to solve nonlinear kinematics problems, has been developed; the method has been successfully applied to serial- and parallel-robot kinematics problems [12, 13].

Likewise, the method has been successfully applied to the five-position Burmester problem [14]. In this paper, we use this method to solve the approximate kinematic-synthesis problem of planar four-bar linkages for rigid-body guidance for more than five poses of the coupler link. This problem consists in finding all the relevant parameters of a four-bar linkage that can produce a sequence of m poses that best approximate, in the least-square sense, a set of $m + 1$ prescribed poses $\{(R_j, \theta_j)\}_0^m$, where R_j and θ_j denote the j th position of a point R of the coupler link and the j th orientation of the same link, respectively, as shown in Fig. 1. Moreover, we assume that $m > 4$, i.e., more than five poses are prescribed, and hence, the m poses cannot be met exactly.

In our approach, symbolic computations are used to reduce the normality conditions of the approximate kinematic synthesis problem to a set of two bivariate equations. These two equations are first plotted in the X_0 - Y_0 plane of Fig. 1, and then overlapped. In principle, their intersections provide, visually, reasonably accurate approximations to all real solutions of the problem under study, i.e., all dyads that verify the normality conditions. Finally, the solutions are refined numerically by means of the Newton-Raphson method to the desired accuracy. A combination of any two real solutions, i.e., of any two of the dyads mentioned above, then may form a four-bar linkage that meets our needs. However, every four-bar linkage thus resulting must undergo further tests to discard unwanted linkages, e. g., those containing branch, order defects [15, 16], or both of them. All computations, plotting, and graphic displays are accomplished using Matlab 4.2, Mathematica 2.0 and AutoCAD 12.0 on a Sun SPARC station IPC.

2 Derivation of the Contour Equations

In Fig. 1, the body under guidance is represented by a trapezoidal block welded to the coupler link, the four-bar linkage being shown at the zeroth pose (R_0, ϑ_0) . It is required to design a four-bar linkage, i.e., to find a pair $(\mathbf{a}_0, \mathbf{b})$ of position vectors of points A_0 and B , respectively, such that the resulting linkage will carry the block through its $m + 1$ prescribed poses, which are given with reference to the coordinate frame O_0 - X_0Y_0 as $\{(R_j, \vartheta_j)\}_0^m$. The two-link chain resulting from the coupling of the coupler link to the BA_j link, or to its $B^*A_j^*$ counterpart, is called a *dyad*. The four-bar linkage is thus obtained by combining two such dyads. Without loss of generality, let us

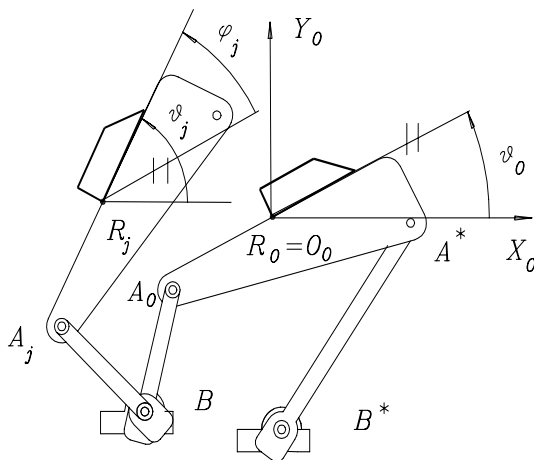


Figure 1: The four-bar linkage and the coordinate system

define the coordinate frame \mathcal{F}_0 with origin at R_0 , as shown in Fig. 1, thereby obtaining $\mathbf{r}_0 = \mathbf{0}$. The condition that the distance between A_0 and B remain constant yields the synthesis equations:

$$\|(\mathbf{r}_j - \mathbf{b} + \mathbf{Q}_j \mathbf{a}_0)\|^2 = \|\mathbf{a}_0 - \mathbf{b}\|^2; \quad j = 1, 2, 3, \dots, m \quad (1)$$

where \mathbf{Q}_j is the matrix rotating the coupler link through an angle φ_j , i.e.,

$$\mathbf{Q}_j = \begin{bmatrix} \cos \varphi_j & -\sin \varphi_j \\ \sin \varphi_j & \cos \varphi_j \end{bmatrix} \quad (2)$$

with $\varphi_j \equiv \vartheta_j - \vartheta_0$. After expanding eq.(1) and simplifying, we obtain

$$f_j \equiv \mathbf{b}^T(\mathbf{1} - \mathbf{Q}_j)\mathbf{a}_0 + \mathbf{r}_j^T \mathbf{Q}_j \mathbf{a}_0 - \mathbf{r}_j^T \mathbf{b} + \frac{\mathbf{r}_j^T \mathbf{r}_j}{2} = 0; \quad j = 1, 2, 3, \dots, m \quad (3)$$

where $\mathbf{1}$ is the 2×2 identity matrix. Since $m > 4$, we cannot find the two vectors \mathbf{a}_0 and \mathbf{b} to satisfy eqs.(3) exactly. However, we can formulate the problem at hand as an optimization problem in order to satisfy those equations as close as possible in the least-square sense, namely,

$$z \equiv \frac{1}{2} \sum_{j=1}^m f_j^2 \quad \rightarrow \quad \min_{\mathbf{a}_0, \mathbf{b}} \quad (4)$$

In order to minimize z , we obtain the normality conditions of this function with respect to the design variables \mathbf{a}_0 and \mathbf{b} , namely,

$$\frac{\partial z}{\partial \mathbf{a}_0} = \sum_{j=1}^m f_j \frac{\partial f_j}{\partial \mathbf{a}_0} = \mathbf{0} \quad (5)$$

$$\frac{\partial z}{\partial \mathbf{b}} = \sum_{j=1}^m f_j \frac{\partial f_j}{\partial \mathbf{b}} = \mathbf{0} \quad (6)$$

where

$$\frac{\partial f_j}{\partial \mathbf{a}_0} = (1 - c_j)\mathbf{b} + s_j \mathbf{E} \mathbf{b} + c_j \mathbf{r}_j - s_j \mathbf{E} \mathbf{r}_j = \mathbf{0} \quad (7)$$

$$\frac{\partial f_j}{\partial \mathbf{b}} = (1 - c_j)\mathbf{a}_0 - s_j \mathbf{E} \mathbf{a}_0 + \mathbf{r}_j = \mathbf{0} \quad (8)$$

with c_j and s_j standing for $\cos \varphi_j$ and $\sin \varphi_j$, and \mathbf{E} defined as

$$\mathbf{E} \equiv \begin{bmatrix} 0 & -1 \\ 1 & 0 \end{bmatrix} \quad (9)$$

Note that f_j is quadratic in the unknowns, its gradient being linear in the same. Hence, the normality conditions constitute a system of four cubic scalar eqs.(5) and (6), which are all functions of the four components of vectors \mathbf{a}_0 and \mathbf{b} . Also note that the first two are linear in \mathbf{a}_0 , while the last two are linear in \mathbf{b} . This feature eases the reduction of the polynomial system to two contour equations.

From eq.(6), we solve for \mathbf{b} in terms of \mathbf{a}_0 symbolically. Then, substituting the expressions thus resulting into eq.(5), we derive two bivariate equations, namely,

$$c_1(\mathbf{a}_0) = 0 \tag{10}$$

$$c_2(\mathbf{a}_0) = 0 \tag{11}$$

each of these equations being nonic in \mathbf{a}_0 .

According to Bezout's Theorem [17], then, the upper bound of the number of solutions is $9 \times 9 = 81$. Although this number appears unusually high, the foregoing equations very likely admit simplifications, that we did not pursue at this stage. Nevertheless, this number is already 1/3 of that reported by [11] in solving an approximate-synthesis problem of a similar complexity. Indeed, the authors of the foregoing reference solved a problem of approximate path generation with prescribed timing of the visited points. Now, a problem of plain path generation can be regarded as one of rigid-body guidance with incompletely-specified poses, for the orientations ϑ_j are not prescribed. If timing is specified, then a correspondence is available between each angular displacement of the input link and the visited point, which, by means of the closure equation of the linkage, allows the analyst to infer the said orientation at each prescribed point. It is thus apparent that the problem solved in [11] is equivalent to the one of rigid-body guidance.

With regard to the number of real and complex solutions to be expected, the Bezout Theorem usually overestimates this number. Tighter bounds are available, as shown in [18], the tightest bound according to this reference being that known as the Bernstein-Khovanskii-Kushnirenko bound, or *BKK bound* for brevity. However, an investigation on the actual number of solutions to the problem at hand is out of the scope of this paper. Further research is needed in the symbolic manipulation of algebraic equations in vector variables, when these equations are formulated in *invariant form*, as

opposed to equations in component form, that would allow the application of the BBK bound to the problem at hand in its present form.

Furthermore, the numerical conditioning of the solutions, which is a measure of the accuracy, and hence, of the reliability, of each real solution, is given by the angle at which the two contours intersect [19]. The most accurate solutions occur at intersections at right angles, while the least at points where the contours are tangent. Apparently, tangent contours are borderline cases where two real solutions merge into one double solution, a case indicating a singularity of the underlying Jacobian matrix.

3 Nature of the Stationary Points

A stationary point is a local minimum, a local maximum, or a saddle point, if the Hessian matrix \mathbf{H} of z with respect to the design vector $\mathbf{x} \equiv [\mathbf{a}_0^T, \mathbf{b}_0^T]^T$ is, correspondingly, negative-semidefinite, positive-semidefinite, or sign-indefinite. We thus have to test the sign-definition of \mathbf{H} , which is given by

$$\mathbf{H} \equiv \begin{bmatrix} \partial^2 z / \partial \mathbf{a}_0^2 & \partial^2 z / (\partial \mathbf{a}_0 \partial \mathbf{b}) \\ [\partial^2 z / (\partial \mathbf{a}_0 \partial \mathbf{b})]^T & \partial^2 z / \partial \mathbf{b}^2 \end{bmatrix} \quad (12)$$

Thus, \mathbf{H} is a *symmetric* block matrix with four 2×2 blocks, each being a partial Hessian. Hence, one of the two off-diagonal blocks is the transpose of the other one. We calculate below the three distinct blocks of eq. (12):

$$\begin{aligned} \frac{\partial^2 z}{\partial \mathbf{a}_0^2} &= \sum_{j=1}^m \frac{\partial f_j}{\partial \mathbf{a}_0} \left(\frac{\partial f_j}{\partial \mathbf{a}_0} \right)^T + \sum_{j=1}^m f_j \frac{\partial^2 f_j}{\partial \mathbf{a}_0^2} \\ \frac{\partial^2 z}{\partial \mathbf{a}_0 \partial \mathbf{b}} &= \sum_{j=1}^m \frac{\partial f_j}{\partial \mathbf{b}} \left(\frac{\partial f_j}{\partial \mathbf{a}_0} \right)^T + \sum_{j=1}^m f_j \frac{\partial^2 f_j}{\partial \mathbf{a}_0 \partial \mathbf{b}} \\ \frac{\partial^2 z}{\partial \mathbf{b}^2} &= \sum_{j=1}^m \frac{\partial f_j}{\partial \mathbf{b}} \left(\frac{\partial f_j}{\partial \mathbf{b}} \right)^T + \sum_{j=1}^m f_j \frac{\partial^2 f_j}{\partial \mathbf{b}^2} \end{aligned} \quad (13)$$

Moreover, from eqs. (7) and (8),

$$\frac{\partial^2 f_j}{\partial \mathbf{a}_0^2} = \mathbf{0}, \quad \frac{\partial^2 f_j}{\partial \mathbf{b}^2} = \mathbf{0}, \quad \frac{\partial^2 f_j}{\partial \mathbf{a}_0 \partial \mathbf{b}} = (1 - c_j) \mathbf{1} + s_j \mathbf{E} \quad (14)$$

Therefore,

$$\begin{aligned} \frac{\partial^2 z}{\partial \mathbf{a}_0^2} &= \sum_{j=1}^m \frac{\partial f_j}{\partial \mathbf{a}_0} \left(\frac{\partial f_j}{\partial \mathbf{a}_0} \right)^T \\ \frac{\partial^2 z}{\partial \mathbf{a}_0 \partial \mathbf{b}} &= \sum_{j=1}^m \frac{\partial f_j}{\partial \mathbf{b}} \left(\frac{\partial f_j}{\partial \mathbf{a}_0} \right)^T + \sum_{j=1}^m f_j \frac{\partial^2 f_j}{\partial \mathbf{a}_0 \partial \mathbf{b}} \\ \frac{\partial^2 z}{\partial \mathbf{b}^2} &= \sum_{j=1}^m \frac{\partial f_j}{\partial \mathbf{b}} \left(\frac{\partial f_j}{\partial \mathbf{b}} \right)^T \end{aligned} \quad (15)$$

4 Example

In this example, the coupler link is to attain 31 prescribed configurations along an elliptical path, which is given in the X_0 - Y_0 plane as

$$\frac{(x+2)^2}{a^2} + \frac{y^2}{b^2} = 1; \quad a = 2; \quad b = 3.5 \quad (16)$$

The 31 points are distributed in cycloidal x -increments along a quarter of the ellipse, the orientations of the coupler following a similar distribution, from 0° to 90° , with $\vartheta_0 = 0$, i.e.,

$$\begin{aligned} s_j &= \frac{j}{m} - \frac{1}{2\pi} \sin\left(\frac{2j\pi}{m}\right) \\ x_j &= -s_j a \\ y_j &= \sqrt{b^2 \left(1 - \frac{(x+a)^2}{a^2}\right)} \\ \varphi_j &= 90^\circ s_j \end{aligned}$$

for $j = 0, 1, 2, \dots, 30$, (x_j, y_j) denoting the \mathcal{F}_0 -coordinates of R_j . Equations (5) and (6) are displayed below, with x_A and y_A denoting the components of vector \mathbf{a}_0 , and similar definitions for x_B and y_B .

$$111.889436614y_A + 139.653932631x_A - 279.316752633y_B + 174.113324453x_B$$

$$\begin{aligned}
&+74.8516326064x_Ax_B - 3.37657168440y_Ay_B - 89.5487609666x_Ay_B + 73.4773525781y_Ax_B \\
&+11.8126390140y_Ax_B^2 + 10.1043403543x_Ax_B^2 + 15.0000219543x_Ay_B^2 - 69.3287757286x_By_B \\
&-23.6252780280x_Ay_Bx_B - 4.89568160000y_Ax_By_B + 21.7329251888x_B^2 + 56.4952351818y_B^2 \\
&\qquad\qquad\qquad -11.8126390140y_Ay_B^2 + 349.662976117 = 0
\end{aligned}$$

$$\begin{aligned}
&128.826867994y_A + 111.889436614x_A - 72.1391586778y_B + 185.559890872x_B \\
&+73.4773525782x_Ax_B + 57.4059441899y_Ay_B - 3.37657168429x_Ay_B + 81.6047759746y_Ax_B \\
&+15.0000219543y_Ax_B^2 + 11.8126390140x_Ax_B^2 - 11.8126390140x_Ay_B^2 - 34.7623099930x_By_B \\
&-4.89568160000x_Ay_Bx_B + 23.6252780280y_Ax_By_B + 26.6286682886x_B^2 - 42.7001074400y_B^2 \\
&\qquad\qquad\qquad +10.1043403543y_Ay_B^2 + 312.185655199 = 0
\end{aligned}$$

$$\begin{aligned}
&185.559890872y_A + 174.113324453x_A - 98.7762946728y_B + 48.0118542891x_B \\
&+43.4658503776x_Ax_B - 34.7623099930y_Ay_B - 69.3287757286x_Ay_B + 53.2573365772y_Ax_B \\
&-11.8126390140x_A^2y_B + 73.4773525781x_Ay_A + 37.4258163031x_A^2 + 40.8023879873y_A^2 \\
&-4.89568160000x_Ay_By_A + 23.6252780280y_Ax_Bx_A + 11.8126390140y_A^2y_B + 15.0000219543y_A^2x_B \\
&\qquad\qquad\qquad +10.1043403543x_A^2x_B + 207.410660253 = 0
\end{aligned}$$

$$\begin{aligned}
&-436.072489107 - 72.1391586778y_A - 279.316752633x_A + 220.46882989y_B \\
&-98.7762946728x_B - 69.3287757286x_Ax_B - 85.4002148800y_Ay_B + 112.990470364x_Ay_B \\
&-34.7623099930y_Ax_B + 15.0000219543x_A^2y_B - 3.37657168420x_Ay_A - 44.7743804833x_A^2
\end{aligned}$$

$$\begin{aligned}
&+28.7029720949y_A^2 - 23.6252780280x_Ay_By_A - 4.89568160000y_Ax_Bx_A + 10.1043403543y_A^2y_B \\
&\qquad\qquad\qquad +11.8126390140y_A^2x_B - 11.8126390140x_A^2x_B = 0
\end{aligned}$$

In pursuing the bivariate contour approach, eqs.(10) and (11) become

$$\begin{aligned}
&.224369587900x_A^9 + (-.927895957000y_A + 6.58632670000)x_A^8 \\
&+ (.897478351000y_A^2 - 21.1110695200y_A + 84.5225510000)x_A^7 \\
&+ (-3.71158382800y_A^3 + 20.6624877000y_A^2 - 200.251585500y_A + 618.289379400)x_A^6 \\
&+ (1.34621752200y_A^4 - 21.4259513000y_A^3 + 109.803976900y_A^2 - 968.683057000y_A \\
&\qquad\qquad\qquad + 2818.85390100)x_A^5 \\
&+ (-5.56737574900y_A^5 - 1.98200170000y_A^4 + 90.7747780000y_A^3 - 30.9935640000y_A^2 \\
&\qquad\qquad\qquad -2402.47783000y_A + 8261.17690000)x_A^4 \\
&+ (.897478345000y_A^6 + 20.4813063000y_A^5 - 58.8750872000y_A^4 + 529.796533000y_A^3 \\
&\qquad\qquad\qquad -1298.21345000y_A^2 - 2569.29130000y_A + 15557.3500300)x_A^3 \\
&+ (-3.71158383000y_A^7 - 39.6061605900y_A^6 + 272.796963100y_A^5 - 356.494081000y_A^4 \\
&+ 503.982020000y_A^3 - 2923.94977000y_A^2 + 373.018040000y_A + 18219.4763000)x_A^2 \\
&+ (.224369584000y_A^8 + 20.7961877300y_A^7 - 84.1565128000y_A^6 + 541.702656000y_A^5 \\
&\qquad\qquad\qquad -670.389238000y_A^4 - 529.794700000y_A^3 - 2489.21282000y_A^2 + 3090.62470000y_A \\
&\qquad\qquad\qquad + 12101.0281690)x_A \\
&-.927895958000y_A^9 - 23.5479972980y_A^8 - 18.2294000000y_A^7 + 147.651699000y_A^6 \\
&+ 536.235673000y_A^5 - 566.351270000y_A^4 - 897.714470000y_A^3 - 697.837120000y_A^2 \\
&\qquad\qquad\qquad + 1888.88431000y_A + 3487.06323000 = 0
\end{aligned}$$

and

$$\begin{aligned}
& -.927895960200x_A^9 + (4.58712207800y_A - 24.6886761030)x_A^8 \\
& + (-3.71158383400y_A^2 + 82.2760364700y_A - 279.762376200)x_A^7 \\
& + (18.3484883160y_A^3 - 77.7793964800y_A^2 + 599.104560910y_A - 1765.07010400)x_A^6 \\
& + (-5.56737575600y_A^4 + 271.279614500y_A^3 - 725.900193000y_A^2 + 2243.08009500y_A \\
& \qquad \qquad \qquad -6793.31782800)x_A^5 \\
& + (27.5227324770y_A^5 - 43.2988754800y_A^4 + 1417.96283050y_A^3 - 3751.88966900y_A^2 \\
& \qquad \qquad \qquad + 4593.82762000y_A - 16439.1814600)x_A^4 \\
& + (-3.71158384900y_A^6 + 295.731119600y_A^5 - 103.005903500y_A^4 + 2733.66754100y_A^3 \\
& \qquad \qquad \qquad -10840.2661700y_A^2 + 5202.88000000y_A - 24817.5212600)x_A^3 \\
& + (18.3484883300y_A^7 + 47.9857339900y_A^6 + 1013.69659300y_A^5 - 888.072249000y_A^4 \\
& + 355.780510000y_A^3 - 16755.2796000y_A^2 + 3678.42311000y_A - 22248.5171000)x_A^2 \\
& + (-.927895959000y_A^8 + 106.727541500y_A^7 + 343.131912100y_A^6 + 635.724595000y_A^5 \\
& - 3223.36020500y_A^4 - 3800.43709400y_A^3 - 12200.4935400y_A^2 + 2664.40390000y_A \\
& \qquad \qquad \qquad -10466.7447470)x_A \\
& 4.58712208100y_A^9 + 38.1938891200y_A^8 + 194.838322120y_A^7 + 141.970397800y_A^6 \\
& - 824.202830000y_A^5 - 3036.34213000y_A^4 - 2486.20998000y_A^3 - 2746.53014000y_A^2 \\
& \qquad \qquad \qquad + 1547.38121000y_A - 1843.87986000 = 0
\end{aligned}$$

The contours defined by the above equations as well as their five intersections are shown in Fig. 2. Finding rough estimates for the real solutions can be done visually with the aid of a mouse; we refined these solutions numerically, as shown in Table 1. This table includes values of the objective function

for each of the five real solutions, along with information on the nature of each stationary point. Since there are five real solutions, there are ten combinations of any two solutions, i.e., there exist 10 possible four-bar linkages that can meet our need. These linkages were then tested for branch and order defects. Those that are defect-free were retained. Two feasible combinations of solutions are available: 3 and 4; and 4 and 5, the latter being shown in Fig. 3 and the coupler link motion in Fig. 4, with the prescribed poses displayed with dashed line. In this figure, we display the prescribed and the attained poses for $j = 0, 2, 6, 8, 10, 12, 14, 16, 18, 21,$ and 30 .

It is noteworthy that the the highest-order terms of the two nonic equations derived above involve one single unknown. Moreover, the coefficients of these terms do not obey any proportionality relation, which means that a degree-reduction is not possible by simple linear combinations, and further investigation is needed to decide whether these polynomials are minimal.

Table 1: The real solutions and their properties

No.	x_A	y_A	x_B	y_B	z	nature
1	-2.81003	0.457322	-3.041139	0.950295	0.22611	saddle
2	-2.08866	0.632387	-2.38149	1.24799	0.690021	saddle
3	-1.28265	0.822615	-2.23162	1.42585	0.66303	saddle
4	-1.06258	-0.251359	-6.21649	-0.130588	0.00570	min.
5	-0.33693	2.53234	-2.48487	2.49868	0.00218	min.

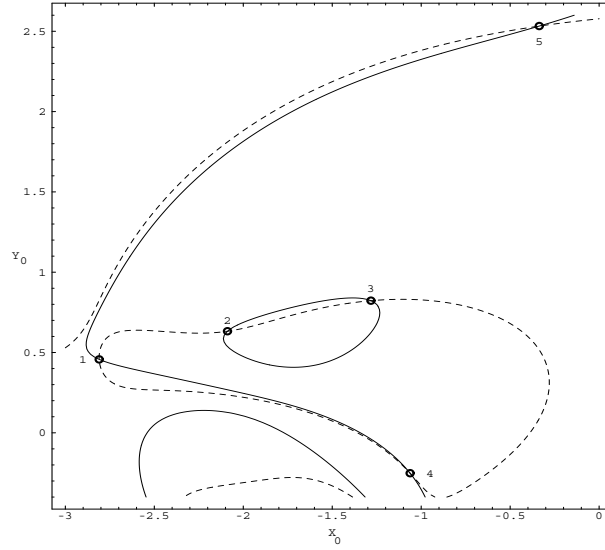


Figure 2: The five intersections of the two contours

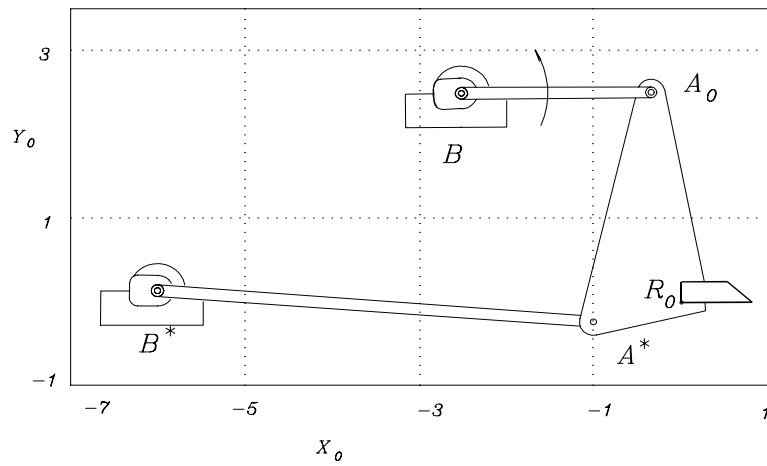


Figure 3: A four-bar linkage generating the prescribed coupler motion with a least-square error

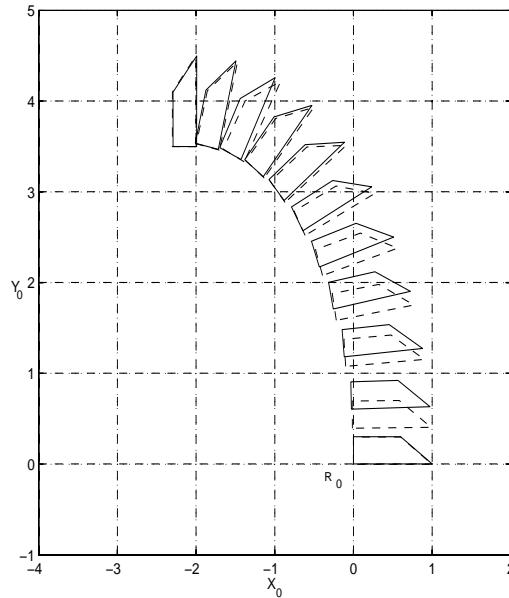


Figure 4: A sample of 11 poses of the motion of the coupler link of the synthesized four-bar linkage, and their prescribed counterparts (in dashed line), for $j = 0, 2, 6, 8, 10, 12, 14, 16, 18, 21,$ and 30

5 Conclusions

The contour method was used to determine all optimum dyads in the approximate synthesis of a planar four-bar linkage for rigid-body guidance. Combining symbolic elimination, modern graphics, and numerical methods, we found all the real solutions visually. An example illustrated the method proposed here, that can be extended to the approximate synthesis of more complex planar and spatial linkages.

We showed that the problem at hand reduces to finding the roots of two nonic equations, the number of possible solutions thus being 81. Further investigation is needed to decide whether this number can be reduced, by application of tighter bounds than the Bezout number, such as the BKK bound.

6 Acknowledgements

The research work reported here was made possible under Research Grant OGP0004532 of the Natural Sciences and Engineering Research Council (NSERC) of Canada. Mr. Yao would like to thank the China Scholarship Program for providing him support during his one-year visit to the Centre for Intelligent Machines, McGill University, Canada.

Calcul de toutes les dyades optimales lors de la synthèse approximative de mécanismes planaires utilisés dans le guidage de bielle

Résumé

La synthèse approximative des mécanismes planaires à quatre barres porte sur le calcul de tous les paramètres significatifs du mécanisme capable de guider sa bielle de façon optimale dans un grand nombre de situations. Nous entendons par “grand” le nombre à partir duquel le mécanisme n’est plus capable de guider la bielle avec précision. Rappelons que l’erreur d’approximation des équations sous-jacentes est définie en terme des moindres carrés, ce qui revient à un problème d’optimisation. Chaque solution, qui correspond à un minimum local d’erreur d’approximation, produit une dyade, la combinaison de deux dyades donnant un mécanisme à quatre barres articulées. Puisque les méthodes purement numériques mènent à des minimums locaux isolés, nous utilisons ici la méthode dite des contours, tout en cherchant à obtenir tous les points stationnaires réels du problème à l’étude. Nous utilisons tout d’abord le calcul formel pour obtenir les *équations normales* du problème d’optimisation. Ces équations sont alors réduites à un ensemble de deux équations polynômiales à deux variables, puis représentées graphiquement dans le plan des deux variables. Les deux contours définis par les équations sont ensuite superposés. En principe, les intersections des contours donnent une représentation visuelle de toutes les solutions réelles du problème ainsi que leur conditionnement numérique. Enfin, nous faisons appel aux méthodes numériques pour affiner les solutions obtenues visuellement et arriver à la précision désirée. La méthodologie décrite est illustrée par un exemple.

7 References

- 1 Morgan, A. P., *Solving Polynomial Systems Using Continuation for Scientific and Engineering Problems*, Prentice-Hall Inc., Englewood Cliffs, 1987.
- 2 Tsai, L. W. and Morgan, A. P., *ASME J. Mechanisms, Transmissions, and Auto. in Design*, 1985, **107** (2), 189–200.
- 3 Lee, H. Y., and Liang, C. G., *Mech. Mach. Theory*, 1988, **23** (3), 219–226.
- 4 Gosselin, C., *Kinematic Analysis, Optimization and Programming of Parallel Robotic Manipulators*, Ph. D. Thesis, Department of Mechanical Engineering, McGill University, Montreal, 1988.
- 5 Nanua, P., Waldron, K. J. and Murthy, V., *IEEE J. Robotics and Automation*, 1990, **6** (4), 438–444.
- 6 Morgan, A. P. and Wampler, C. W., *ASME J. Mechanical Design*, 1990, **112**, 544–550.
- 7 Wampler, C. W., Morgan, A. P. and Sommese, A. J., *ASME J. Mechanical Design*, 1990, **112** (1), 59–68.
- 8 Raghavan, M. and Roth, B., *ASME J. Mechanical Design*, 1993, **115**, 502–508.
- 9 Raghavan, M., *ASME J. Mechanical Design*, 1993, **115**, 277–282.
- 10 Erdmann, A. G. (editor), *The First Forty Years of Modern Kinematics. A Tribute to Ferdinand Freudenstein*, John Wiley and Sons, Inc., New York, 1992.


- 11 Liu, A. and Yang, T., *Proc. Inter Conf. Mechanical Transmissions and Mechanisms*, Tianjin, China, 1997, 131–135.
- 12 Zanganeh, K. E. and Angeles, J.,  *Computational Kinematics*, in J. Angeles, Hommel, G. and Kovács, P. (eds.), Kluwer Academic Publishers, 1993, 165–173.
- 13 Zanganeh, K. E., *The Contour Method: An Interactive Approach to the Inverse Kinematics of Serial Manipulators*, Department of Mechanical Engineering and Centre for intelligent Machines, Technical Report TR-CIM-97-10, McGill University, Montreal, 1997.
- 14 Chang, C.-Y., Angeles, J. and González-Palacios, M. A., *Proc. 1991 ASME Design Automation Conference. Advances in Design Automation*, Miami, 1991 **2**, 321–326.
- 15 Tinubu, S. O. and Gupta, K. C., *ASME J. Mechanisms, Transmissions, and Auto. in Design*, 1984, **106**, 348–354.
- 16 Waldron, K. J. and Stevensen, E. N., *ASME J. Mechanical Design*, 1979, **101**, 428–437
- 17 van der Waerden, B. L., *Algebra*, Vols. 1,2, Translated by F. Blum and J. Schulenberger, Frederick Ungar Pub. Co., New York, 1970.
- 18 Nielsen, J. and Roth, B., “Formulation and solution for the direct and inverse kinematics problems for mechanisms and mechatronics systems”, in Angeles, J. and Zakhariiev, E. (eds.), NATO ASI Series F, Vol. 161, Springer-Verlag, Heidelberg, 1997, 233–252.
- 19 Angeles, J., *Fundamentals of Robotic Mechanical Systems. Theory, Methods, and Algorithms*, Springer-Verlag, New York, 1997.

Figure Legends

Figure 1: The four-bar linkage and the coordinate system

Figure 2: The five intersections of the two contours

Figure 3: A four-bar linkage generating the prescribed coupler motion with a least-square error

Figure 4: A sample of 11 poses of the motion of the coupler link of the synthesized four-bar linkage, and their prescribed counterparts (in dashed line), for $j = 0, 2, 6, 8, 10, 12, 14, 16, 18, 21,$ and 30

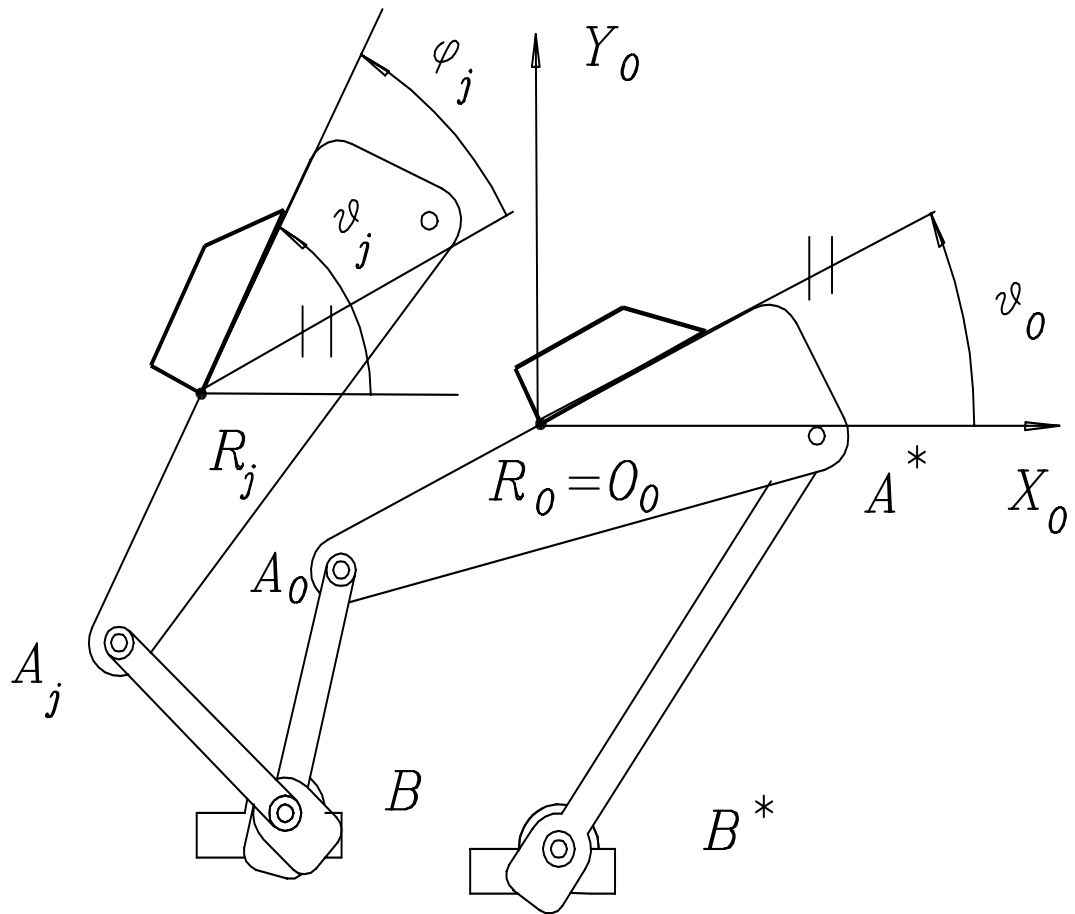


Figure 1: The four-bar linkage and the coordinate system

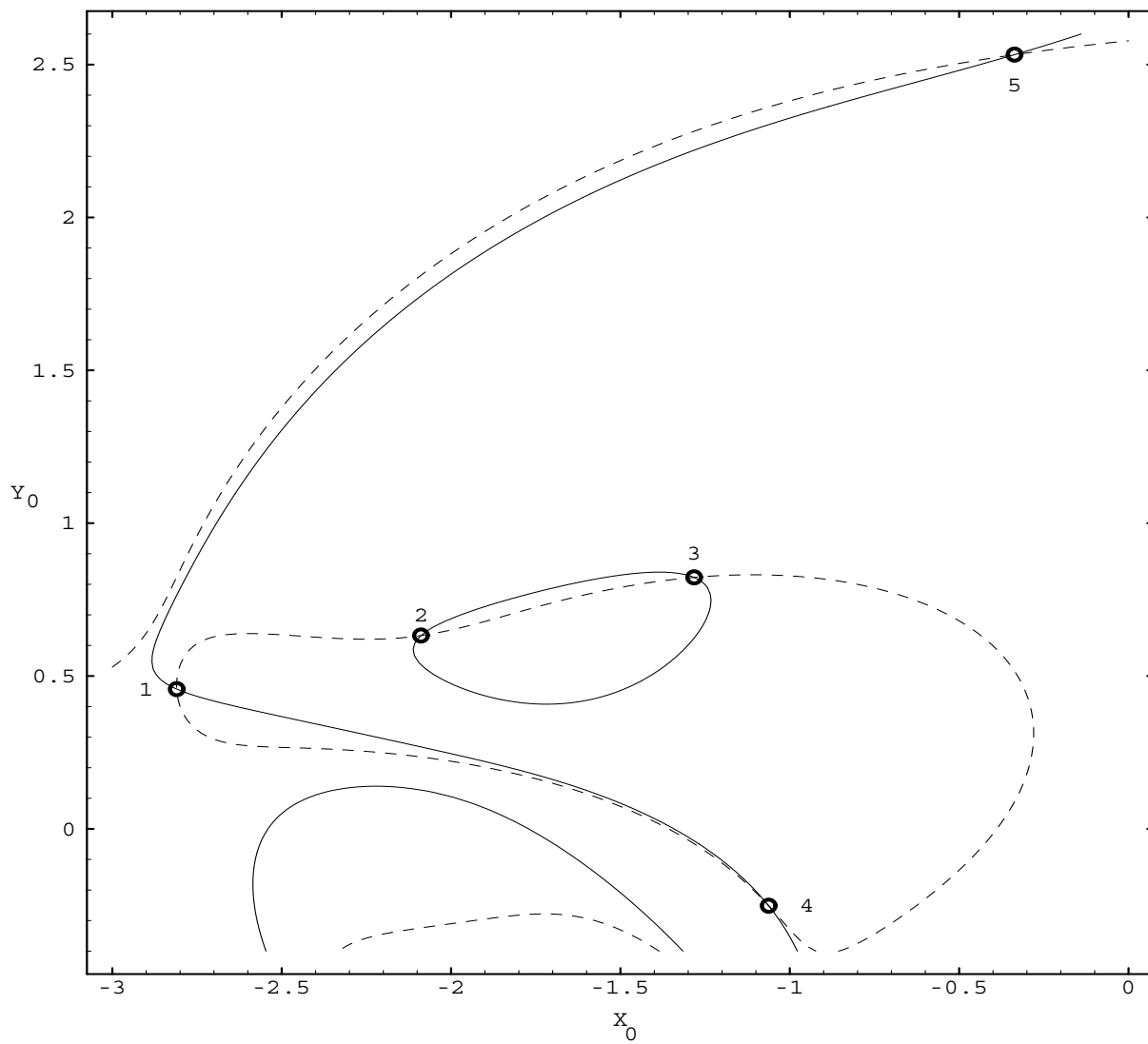


Figure 2: The five intersections of the two contours

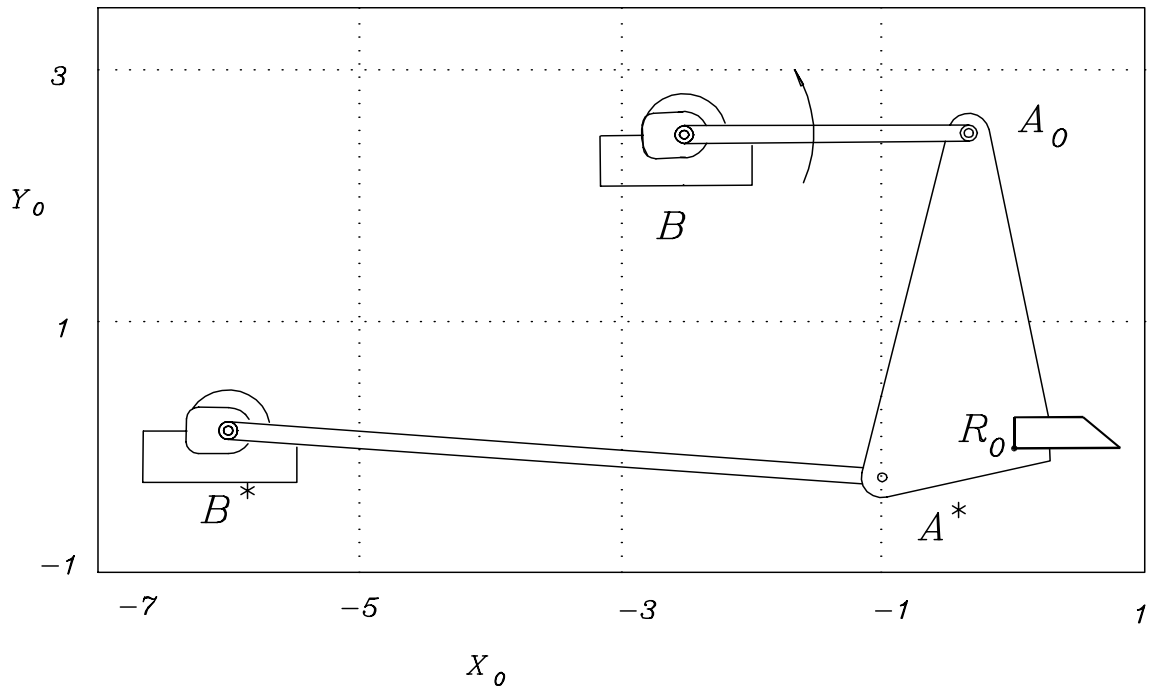


Figure 3: A four-bar linkage generating the prescribed coupler motion with a least-square error

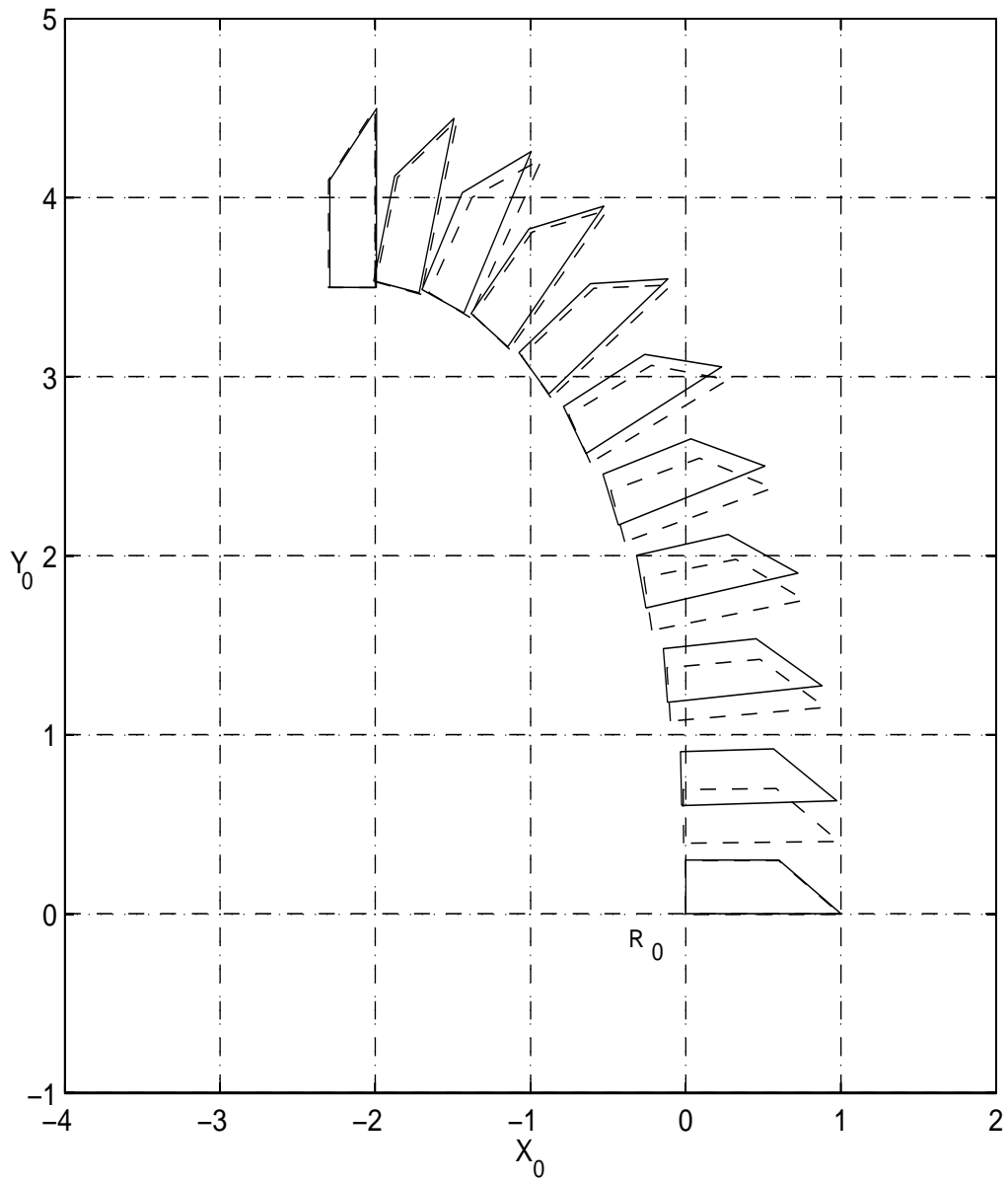


Figure 4: A sample of 11 poses of the motion of the coupler link of the synthesized four-bar linkage, and their prescribed counterparts (in dashed line), for $j = 0, 2, 6, 8, 10, 12, 14, 16, 18, 21,$ and 30